

The Properties of the Metal Complex Hydrides

Ab initio Calculation of Geometric Structure, Electronic Charge Distribution and Binding Energy of LiBH_4 , NaBH_4 , LiAlH_4 , and NaAlH_4

Rosanna Bonaccorsi, Eolo Scrocco, and Jacopo Tomasi

Laboratorio di Chimica Quantistica ed Energetica Molecolare del C.N.R., Via Risorgimento, 35, I-56100, Pisa, Italy

The essential features (geometries of the minima and of the saddle points, energy barriers) of the potential energy surface of the four hydrides YXH_4 mentioned in the title have been determined with two basis sets, of minimal and DZ quality respectively. The importance of the different extent of the deformation of the XH_4 group in the different structures of the four hydrides is brought out and discussed. The aspects of charge distribution and bonding are examined drawing on population analysis, comparison of the electrostatic molecular potentials and decomposition of the interaction energy (this last referred to the $\text{Y}^+ + \text{XH}_4^- \rightarrow \text{YXH}_4$ process). The capability of XH_3 in effecting the etherolytic disruption of the $\text{Y}-\text{H}$ bond is finally brought out.

Key words: Metal hydrides, bonding properties of \sim – Interaction energy decomposition – Catalytic effects on heterolytic cleavage

1. Introduction

The mechanism of the carbonyl reduction with the complex metal hydrides mentioned in the title is not yet completely assessed. In particular there are some indirect indications suggesting differences in the chemical behaviour of the different hydrides which deserve a careful determination [1–5]. Within the frame of a study of these mechanisms, undertaken in our laboratory, we present here a preliminary report on the electronic structure of the isolated reagents.

The attention is focussed on the essential features of the potential energy surface (position and relative value of the minima and of the barriers), on the characteristics of the bonding between the alkali atom and the other moiety of the molecule, on the differences in the heterolytic dissociation energies along our set of complex hydrides. The calculations have been performed with two different basis sets; a

minimal set, easier to handle in following studies of the reaction mechanism with realistic models of the organic substrate but not adequate to reproduce well the energetics of the dissociation processes, and a second set, of DZ quality, simple enough to be used also for the calculation of some selected points of the energy hypersurface of the composite system hydride–organic substrate and flexible enough to give a reasonable account of the energies involved in the dissociation processes.

The analyses reported here refer only to the isolated molecules (the effect of appropriate solvents on the structure of the hydrides will be dealt with in a future paper) but they certainly are of some interest *in se*, owing to the chemical importance of such molecules, not yet well studied even under gas phase conditions. In fact the *ab initio* studies we know on the outstanding characteristics of the potential energy surface of these hydrides concern only the LiBH_4 molecule [6–7].

2. Results and Discussion

For the calculation of the SCF MO-LCAO electronic wavefunction, performed with the Gaussian 70 package [8] we have employed the STO-3G basis set [9] and a contracted Gaussian set of double zeta quality proposed by Huzinaga [10] on the basis of its uncontracted set (14s, 6p; 14s, 7p; 11s, 6p; 11s; 4s) (for Al, Na, B, Li, and H in this order).

For each metal hydride we have determined with the STO-3G basis rather larger portions of the ground state potential energy hypersurface which will be used later in the continuation of this study. We limit ourselves to reporting here the results for the points corresponding to the equilibrium geometry and a few other points of particular relevance.

The four molecules can be roughly described as distorted XH_4 groups (X stands for B and Al) interacting with the Y atom (Y stands for Li and Na). Three relevant structures are depicted in Fig. 1. Structure I corresponds (with one exception, see later) to the most stable geometrical arrangement; this structure has a C_{3v} sym-

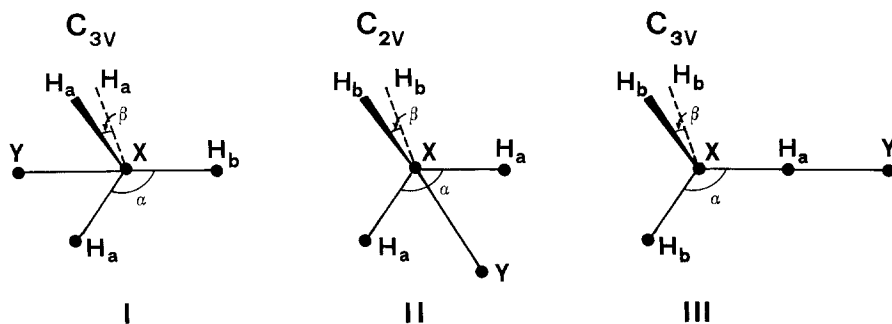


Fig. 1. Geometrical arrangement of the three structures of the YXH_4 compounds considered in this paper

Table 1. Geometries and energies of the three more stable structures of the complex hydrides YXH_4 calculated with the STO-3G basis set

	Structure	R_{YX}^a	R_{XH_a}	$R_{XH_b}^a$	α^b	β^b	E^c	ΔE^d
LiBH ₄	I	1.87	1.23	1.15	113.3	105.3	-34.0025	0
	II	2.06	1.27	1.16	106.8	115.3	-33.9920	6.59
	III	2.92	1.39	1.16	104.1	115.2	-33.9508	32.44
NaBH ₄	I	2.18	1.19	1.16	111.0	107.9	-186.5652	0
	II	2.36	1.21	1.16	109.6	114.2	-186.5628	1.51
	III	2.92	1.20	1.17	106.5	112.3	-186.5350	18.95
LiAlH ₄	I	2.05	1.61	1.46	124.3	91.4	-248.6692	0
	II	2.34	1.71	1.47	87.7	124.0	-248.6667	1.57
	III	3.26	1.74	1.49	100.1	117.0	-248.6051	40.23
NaAlH ₄	I	2.35	1.53	1.48	118.5	99.1	-401.1749	4.77
	II	2.59	1.56	1.49	96.0	120.0	-401.1825	0
	III	3.28	1.57	1.50	103.4	114.8	-401.1556	16.88

^a In Å.^b In degrees.^c In hartrees.^d In kcal/mole.

metry and there are, in fact, four equivalent reciprocal arrangements of the XH_4 and Y groups. The top of the barrier for the passage from one to another of these minima is given by structure II (symmetry C_{2v}). On the top of the barrier the interaction between XH_4 and Y is not supported by three H atoms, as it is in the case of structure I, but by two atoms only. Structure III (symmetry C_{3v}) corresponds to the best geometrical arrangement in which the interaction is supported by one H atom. This last structure does not play an important role in the geometry rearrangements of the metal hydrides in the gas phase, but its importance increases in solution and in the carbonyl reduction mechanism as our preliminary studies on the influence of the solvent indicate, and as the discussion on the experimental data on the reaction mechanism suggests. In a recent paper Dill *et al.* [6] consider also in the $LiBH_4$ case two other structures, both corresponding to a LiH group linked to BH_3 via the Li atom, but they are higher in energy than those we have considered here.

The energies and the numerical values of the geometrical parameters of the structures outlined above, obtained with the STO-3G basis, are reported in Table 1. The results of the geometry optimization for structures I and II (obtained with the DZ basis set) are given in Table 2 (we have not considered it necessary to optimize also structure III with this second basis set). In Table 3 we give also the optimized geometries and energies, obtained with both basis sets, for the separate closed-shell fragments in which such complex molecules can be reasonably partitioned (i.e. XH_4^- and Y^+ , XH_3 and YH).

According to the STO-3G results structure I is more tightly bound than structure II: in I the X-Y distance is smaller and also the R_{XH} values are smaller. In both structures the distances between the central X atom and the hydrogen atoms which support the interaction with Y (R_{XH_a}) are larger than the distances with the other H atoms (R_{XH_b}).

Table 2. Geometries and energies of the two more stable structures of the complex hydrides YXH_4 calculated with the DZ basis set

	Structure	R_{YX}^a	$R_{XH_a}^a$	$R_{XH_b}^a$	α^b	β^c	E^c	ΔE^d
LiBH ₄	I	2.06	1.25	1.20	113.3	105.3	-34.4158	0
	II	2.21	1.28	1.21	106.8	115.3	-34.4118	2.51
NaBH ₄	I	2.38	1.26	1.21	111.0	107.9	-188.8259	0
	II	2.50	1.27	1.22	109.6	114.2	-188.8218	2.57
LiAlH ₄	I	2.50	1.70	1.61	124.3	91.4	-251.6072	0
	II	2.66	1.73	1.62	87.7	124.0	-251.6105	2.07
NaAlH ₄	I	2.70	1.68	1.63	118.5	99.1	-406.0229	0.50
	II	2.94	1.72	1.63	96.0	120.0	-406.0237	0

^a In Å. ^b In degrees. ^c In hartrees. ^d In kcal/mole.

These two structures can be safely viewed as deriving from an interaction between a distorted XH_4^- anion and a Y^+ cation. This interaction reduces the value of R_{XH} in the complex with respect to the value found in BH_4^- and AlH_4^- . The angular distortion is larger in the AlH_4^- case and, for the same XH_4^- group, is larger when $Y = Li$.

Structure III could be viewed also as deriving from the interaction of XH_3 with YH . According to this point of view one can observe from the data of Table 1 that the interaction produces a shortening of the XH_b distances (with respect to XH_3), while R_{YH_a} is larger than in YH . The angular distortion is larger for the BH_3 group than for the AlH_3 group.

On the whole, the geometrical structures seem to be reasonable and in agreement with intuition.

The values obtained with the Huzinaga's basis show the same trend. The DZ basis set gives consistently larger X-H distances, while the angular parameters are

Table 3. Geometries and energies of some closed-shell fragments of the YXH_4 systems

	STO-3G		DZ	
	R (Å)	E (a.u.)	R (Å)	E (a.u.)
H ⁻		-0.1586		-0.4481
Li ⁺		-7.1354		-7.2363
Na ⁺		-159.7846		-161.6697
LiH	1.515	-7.8634	1.645	-7.9691
NaH	1.666	-160.3157	1.863	-162.3763
BH ₃ ^a	1.180	-26.0699	1.190	-26.3724
AlH ₃ ^a	1.501	-240.7276	1.625	-243.5661
BH ₄ ^{-b}	1.188	-26.5531	1.254	-26.9612
AlH ₄ ^{-b}	1.518	-241.1673	1.685	-244.1825

^a D_{3h} symmetry.

^b T_d symmetry.

surprisingly equal in the two sets of calculations (deviations of less than 0.5 degrees).

Both basis sets indicate structure I as the more stable in LiBH_4 , NaBH_4 , LiAlH_4 and structure II in NaAlH_4 .

The energy barriers separating the equivalent minima of each hydride does not present the same trend along the set of molecules in the two sets of calculations. The highest barrier corresponds to the LiBH_4 molecule in the STO-3G basis (6.5 kcal/mole), while in the DZ basis the corresponding value is decidedly lower (2.5 kcal/mole). We recall that Dill *et al.* [6] obtain for this molecule a barrier of 5.4 kcal/mole with 6-31G* calculations performed at the STO-3G geometries, while Boldyrev *et al.* [7] obtain 3.9 kcal/mole with a geometry optimization performed on a basis set of DZ quality and 4.5 kcal/mole with a basis set including polarization functions (this last value corresponds to calculations performed with the geometry of the BH_4 fragment kept fixed and equal to that of an isolated BH_4^- ion).

The relative importance of the distortion of the XH_4 fragment in the different hydrides and in the different structures of each hydride can be appreciated by examining the data collected in Table 4. Such data concern the difference in energy between the HX_4^- anion at its equilibrium geometry (see Table 3) and at the geometries corresponding to those of the XH_4 fragments in the different structures of the complex hydrides. These results confirm what has been said above, namely that the STO-3G basis emphasizes in general the distortion, and that the distortion effects are larger when $\text{Y} = \text{Li}$ and $\text{X} = \text{Al}$.

The approximation of using a rigid geometry for the XH_4 group in the complex hydrides can give rise to incorrect estimations of the relative stabilities of the different structures. In Table 5 we give the energies of the hydrides calculated by keeping the internal geometry of the XH_4 group rigid and equal to that of XH_4^- ; the introduction of this approximation modifies the trend of the relative energies, and, in particular, produces an inversion of the position of the minimum and of the saddle point in both basis sets.

Another approximation in the calculation of the relative stability of the different structures could be represented by the use of geometries optimized with a minimal basis also for calculations with larger basis sets. In the present case this approximation can be used with confidence for LiBH_4 , but introduces sizable errors in the

Table 4. Differences between the energy of the XH_4^- ion at its equilibrium geometry and at the geometries present in the different structures of the YXH_4 compounds (kcal/mole)

Structure	STO-3G			DZ	
	I	II	III	I	II
LiBH_4	-4.46	-5.99	-6.62	-1.36	-1.29
NaBH_4	-0.26	-1.00	-0.95	-0.37	-0.77
LiAlH_4	-31.43	-28.04	-17.87	-13.74	-7.94
NaAlH_4	-9.64	-6.56	-4.48	-5.11	-3.43

Table 5. Energies and geometries of the more important structures of the YXH_4 compounds determined with the constraint of keeping rigid the internal geometry of the XH_4 fragment^a

	Structure	STO-3G			DZ		
		R_{YX}^b	E^c	ΔE^d	R_{YX}^b	E^c	ΔE^d
LiBH ₄	I	1.87	-33.9974	0	2.06	-34.4144	0
	II	2.06	-33.9852	7.66	2.20	-34.4100	2.76
	III	2.70	-33.9393	36.46			
NaBH ₄	I	2.19	-186.5641	0	2.37	-188.8248	0
	II	2.35	-186.5612	1.82	2.52	-188.8205	2.70
	III	2.92	-186.5327	19.70			
LiAlH ₄	I	2.02	-248.6291	2.95	2.54	-251.5870	4.20
	II	2.21	-248.6338	0	2.63	-251.5937	0
	III	3.04	-248.5820	32.51			
NaAlH ₄	I	2.34	-401.1581	8.79	2.79	-406.0095	2.70
	II	2.47	-401.1721	0	2.90	-406.0138	0
	III	3.25	-401.1492	14.37			

^a The internal geometries of the BH₄ and AlH₄ fragments are equal to those of BH₄⁻ and AlH₄⁻ reported in Table 3.

^b In Å. ^c In hartrees. ^d In kcal/mole.

other molecules. In fact the ΔE values between structures II and I, calculated with the DZ basis on the STO-3G geometries are: 2.3, 0.9, -7.0 and -4.8 kcal/mole (compare with the corresponding values given in Table 2 in the same order). Also in this approximation there is in LiAlH₄ an inversion between minimum and barrier.

Passing now on to compare the description of the electron distribution provided by the two basis sets, it appears from the results of the population analysis given in Table 6 that the Huzinaga's basis tends to give a larger charge separation (and a larger dipole moment) than the STO-3G one. We recall that there is a general trend of the STO-3G basis to give lower dipole moments (with respect to DZ bases) at least for first-row molecules. Little is known about the relative merit of these bases for molecules containing Na and Al atoms.

According to the population analysis, in the DZ wavefunctions there is a sharp charge separation between the two fragments, XH₄ and Y, which could be indicated, in a fairly good approximation, as ions with formal charge -1 and +1, respectively. This charge separation is far from complete in the STO-3G wavefunctions. Particularly striking is the case of LiAlH₄: the formal charge of the Li atom in structure I is negative. In order to look into the features of the charge distribution more accurately one can resort to the examination of the electrostatic potential maps. The electrostatic potential maps give a detailed image of the spatial features of the charge distribution clearer than the total electronic density maps [11]. By comparing Figs. 2 and 3 (the first is a map of the electrostatic potential of LiAlH₄ in the STO-3G basis, the second a map for the same molecule in the DZ basis) it is evident that the difference in the two charge distributions is not so drastic as one

Table 6. Dipole moments and formal atomic charges according to the Mulliken population analysis

Structure	STO-3G						DZ					
	Y	X	H _a	H _b	μ (debyes)		Y	X	H _a	H _b	μ (debyes)	
LiBH ₄	I	0.32	-0.04	-0.07	-0.07	5.05	1.01	-0.86	-0.09	0.12	8.33	
	II	0.35	-0.02	-0.08	-0.08	5.87	0.99	-0.79	-0.18	0.08	8.74	
	III	0.50	-0.02	-0.11	-0.12	9.33						
NaBH ₄	I	0.87	-0.16	-0.20	-0.12	9.01	0.98	-0.82	-0.08	0.09	10.07	
	II	0.85	-0.13	-0.22	-0.14	9.60	0.97	-0.77	-0.16	0.06	10.37	
	III	0.87	-0.10	-0.27	-0.17	12.11						
LiAlH ₄	I	-0.21	1.01	-0.24	-0.19	1.01	1.05	-0.04	-0.33	-0.03	7.09	
	II	-0.10	0.97	-0.16	-0.27	2.81	1.01	0.11	-0.46	-0.10	8.03	
	III	0.30	0.83	-0.14	-0.33	8.67						
NaAlH ₄	I	0.82	0.72	-0.41	-0.32	7.55	1.03	-0.05	-0.30	-0.07	9.50	
	II	0.78	0.73	-0.42	-0.34	8.67	0.99	0.07	-0.40	-0.13	10.50	
	III	0.82	0.74	-0.45	-0.37	12.17						

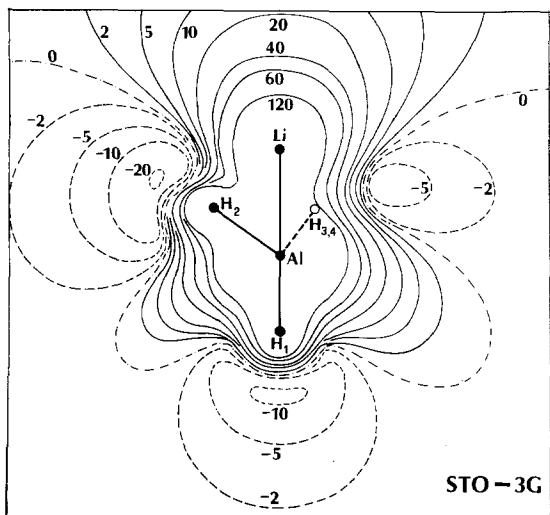


Fig. 2. Electrostatic potential maps for structure I of LiAlH_4 (STO-3G basis). The values of the isopotential lines are given in kcal/mole

could judge from the population analysis. In fact in both cases the Li atom acts as a positively charged counterpart of the AlH_4 group which gives, on the whole, negative contributions to the electrostatic potential. Other features of these maps are of some interest, in particular the location of the negative minima (i.e. of the most favoured positions, on the electrostatic basis, for an attack of a positively charged reactant). These minima in fact are placed in correspondence to the H atoms, while in general near the H atoms the electrostatic potential is positive and the minima are placed in intermediate regions (see, e.g., Ref. [12] which concerns

mainly the CH_2 and $-\text{CH}_3$ groups). It may be added that the electrostatic maps

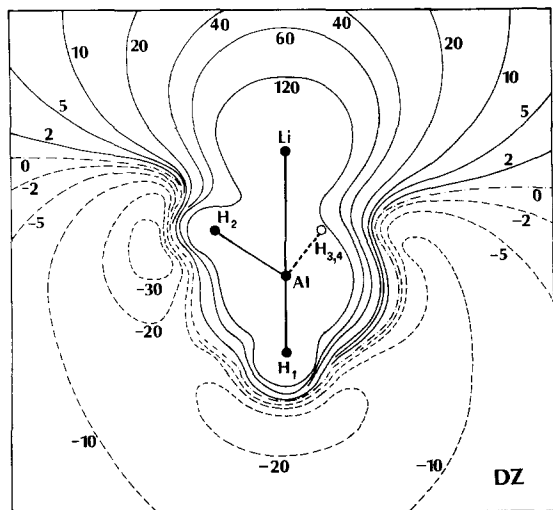


Fig. 3. Electrostatic potential map for structure I of LiAlH_4 (DZ basis)

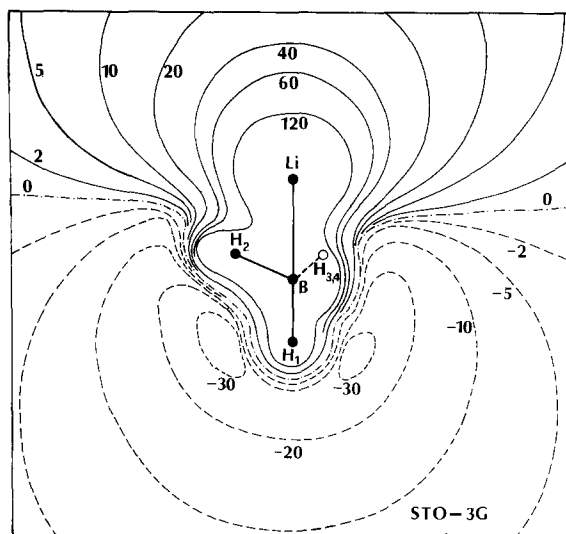


Fig. 4. Electrostatic potential map for structure I of LiBH_4 (STO-3G basis)

of hydrides containing the BH_4 group (see Figs. 4 and 5) show the usual shape of the potential, i.e. with minima along the bisector line of the HBH angles. The corresponding maps for the compounds containing the Na atom (not reproduced here, but available upon request to the authors) indicate that the electrostatic potential near the XH_4 group is more negative, in agreement with the larger dipole moment of these compounds.

The inadequacy of the population analysis for getting an estimation of the charge distribution characteristics, and, of consequence, also of the bonding characteristics of a compound, also appears from the examination of the interaction energy analysis. We report in Table 7 the decomposition of the interaction energy between

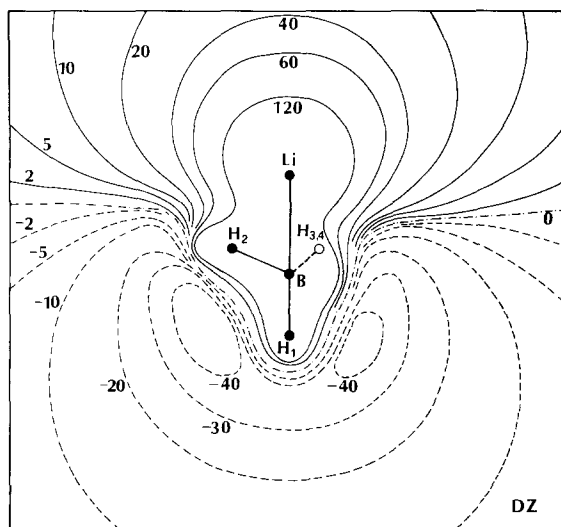


Fig. 5. Electrostatic potential map for structure I of LiBH_4 (DZ basis)

XH_4^- and Y^+ performed with the Morokuma's technique [13]. The energy of the whole system AB is considered as composed of the energy of the two separate partners A and B, plus an interaction term ΔE which is decomposed in a few terms of clear intuitive meaning:

$$\Delta E_{\text{SCF}} = E(\text{AB})_{\text{SCF}} - (E(\text{A})_{\text{SCF}} + E(\text{B})_{\text{SCF}}) = E_{\text{es}} + E_{\text{pol}} + E_{\text{ex}} + E_{\text{ct}}. \quad (1)$$

The first term, E_{es} , gives the electrostatic interaction energy between the two rigid partners A and B, the second, E_{pol} , the mutual polarization energy of A and B, the third the non-classical exchange terms and the last the charge transfer contributions to the interaction energy. For the operational definition of such terms and for their interpretation we refer to the relatively abundant literature on this subject (see e.g. [13–16]). The partition of ΔE given in Table 7 indicates that the classical terms ($E_{\text{es}} + E_{\text{pol}}$) are the dominant ones, but, at the same time, that the charge transfer term is far from negligible. Compare, for example, with the decompositions of the interaction energy of a metallic cation with small neutral molecules [16–17], which gives, in general, values of E_{ct} decidedly smaller. For all the species, and for all the geometries here considered the bond cannot be considered as purely ionic.

The data of Table 7 refer to the geometries given in Tables 1 and 2 for the metal hydrides as well as for the separate partners XH_4^- . In other words we have not employed in the calculation of ΔE the energy of the unperturbed T_d structure of the XH_4^- anions, but a geometry equal to that of the XH_4 fragment in the molecule disregarding thus the deformation contribution to the interaction energy already considered in Table 4.

This separation, somewhat arbitrary, of the deformation energy contributions does not alter the results of the interaction energy analysis. We give in Table 8 the decomposition of ΔE performed on the structures considered in Table 5, i.e. on structures which maintain the rigid structure of the XH_4^- anions. It may be of some interest that the relative weight of each separate contribution to ΔE (i.e. the value of $E_i/\Delta E$, where the E_i 's are the four contributions given in Eq. (1)) remains remarkably constant in passing from the energy decompositions of Table 7 to those of Table 8. Noticeably more different are the values of $E_i/\Delta E$ calculated in the two basis sets; in particular the larger value of $E_{\text{es}}/\Delta E$ and the smaller value of $E_{\text{pol}}/\Delta E$ in the DZ basis correspond to the higher ionic character these compounds have in the DZ SCF description.

As was said in the introduction we shall not consider in this paper the features of the actual mechanism of reaction which are still under discussion. We limit ourselves to remark that in all proposed mechanisms there is a heterolytic cleavage of a Y—H bond. It may be of some interest to obtain, from the data presented above, an appraisal of the “intrinsic” (i.e. without intervention of the solvent and of the organic substrate) capabilities of the different metal hydrides to get the heterolytic dissociation. The relevant data are presented in graphical form in Figs. 6 and 7.

The selection of the reference states adopted in these two figures emphasizes the effect of the formation of the complex metal hydride starting from the simple hydrides YH and XH_3 . It appears quite evident that the complex hydrides have a

Table 7. Decomposition of the interaction energy for the more stable structure (values in kcal/mole)

Structure	STO-3G						DZ					
	ΔE	E_{es}	E_{pot}	E_{ex}	E_{ot}	ΔE	E_{es}	E_{pot}	E_{ex}	E_{ot}		
LiBH ₄	I	-201.46	-168.63	-6.07	29.17	-55.92	-138.32	-149.58	-14.31	34.65	-9.08	
	II	-196.40	-163.54	-4.69	26.11	-54.29	-135.77	-149.42	-10.89	33.25	-8.72	
	III	-170.31	-130.47	-9.84	21.10	-51.10						
NaBH ₄	I	-142.98	-150.80	-3.84	25.89	-14.23	-122.73	-138.32	-10.71	31.88	-5.58	
	II	-142.22	-145.61	-3.13	23.95	-17.43	-120.56	-138.64	-8.94	33.00	-5.99	
	III	-124.77	-122.40	-6.54	21.30	-17.13						
LiAlH ₄	I	-261.43	-175.52	-6.65	30.91	-110.16	-132.20	-134.83	-15.71	31.16	-12.82	
	II	-256.42	-170.55	-6.68	29.27	-108.46	-128.50	-135.52	-14.77	34.58	-12.79	
	III	-207.61	-137.38	-11.09	24.00	-83.14						
NaAlH ₄	I	-149.57	-147.08	-4.25	25.43	-23.67	-112.49	-124.36	-14.85	34.91	-8.20	
	II	-151.25	-144.08	-4.00	25.27	-28.44	-111.29	-124.07	-9.91	30.24	-7.56	
	III	-132.30	-124.91	-7.68	25.85	-25.57						

Table 8. Decomposition of the interaction energy for structures calculated with internal geometry of the XH_4 group kept equal to that of the XH_4 anion (values in kcal/mole)

Structure	STO-3G					DZ					
	ΔE	E_{res}	E_{pol}	E_{ex}	E_{ot}	ΔE	E_{res}	E_{pol}	E_{ex}	E_{ot}	
LiBH_4	I	-193.83	-162.54	-6.75	27.20	-51.73	-136.08	-145.92	-15.17	34.35	-9.34
	II	-186.14	-158.30	-4.73	23.93	-47.04	-133.34	-144.80	-11.09	31.32	-8.77
	III	-157.37	-127.94	-9.03	20.09	-40.49					
NaBH_4	I	-142.06	-148.48	-4.02	24.88	-14.44	-121.67	-136.37	-10.99	31.43	-5.74
	II	-140.21	-143.91	-3.30	23.74	-16.74	-118.95	-135.69	-9.31	32.24	-6.19
	III	-122.33	-120.70	-6.53	21.13	-16.23					
LiAlH_4	I	-204.82	-125.61	-7.57	19.91	-91.55	-105.80	-105.39	-16.47	26.80	-10.74
	II	-207.77	-132.73	-3.98	13.42	-84.48	-110.00	-113.54	-9.86	21.70	-8.30
	III	-175.28	-124.72	-10.14	22.45	-62.87					
NaAlH_4	I	-129.41	-121.48	-4.65	18.26	-21.54	-98.94	-106.72	-16.00	31.34	-7.56
	II	-138.22	-125.51	-3.02	15.76	-25.45	-101.66	-110.05	-8.24	22.77	-6.14
	III	-123.83	-118.36	-7.72	25.52	-23.27					

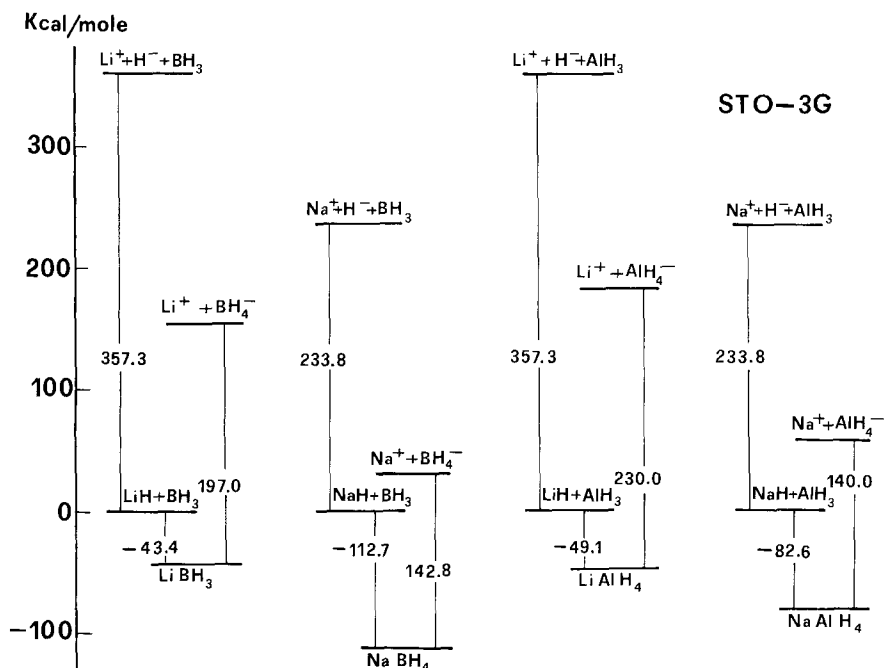


Fig. 6. Diagrams of the energies involved in the heterolytic dissociations of the Y—H bonds (STO-3G calculations)

larger intrinsic capability than YH of undergoing the heterolytic dissociation. This influence of XH_3 on the intrinsic properties of YH can be heuristically called, as in our preceding papers [18–20], the “catalytic” effect of XH_3 .

The STO-3G basis gives unrealistic (i.e. too high) dissociation energies and this defect is particularly evident in the LiH case (the experimental dissociation energies, measured from the bottom of the potential energy curve, are of the order of 164.9 for LiH and 154.5 kcal/mole for NaH, while the corresponding values at the Hartree-Fock limit are 165.0 and 143.1 kcal/mole),¹ while in the complex hydrides the magnitude of the errors due to the limitation of the basis set are presumably lower (to our knowledge, there are no reliable estimates of the experimental values of the heterolytic dissociation in the gas phase of the YXH_4 species).

More reliable are the values obtained with the Huzinaga’s basis. DZ bases give a reasonable prediction of the energy for the process $\text{HY} \rightarrow \text{H}^+ + \text{Y}^-$ in halogenic acids in absence as well as in presence of small complexing molecules, like H_2O or HY [20]. In the present case the absolute error is somewhat larger, owing to the rather poor description of H^- , but we feel that the trend of the energies in the set of chemical processes here considered is passably reproduced.

According to the DZ results the catalytic effect of AlH_3 is larger than that of the BH_3 in depressing the heterolytic dissociation energy of the YH bond.

¹ The relevant data are taken from Refs. [21–23].

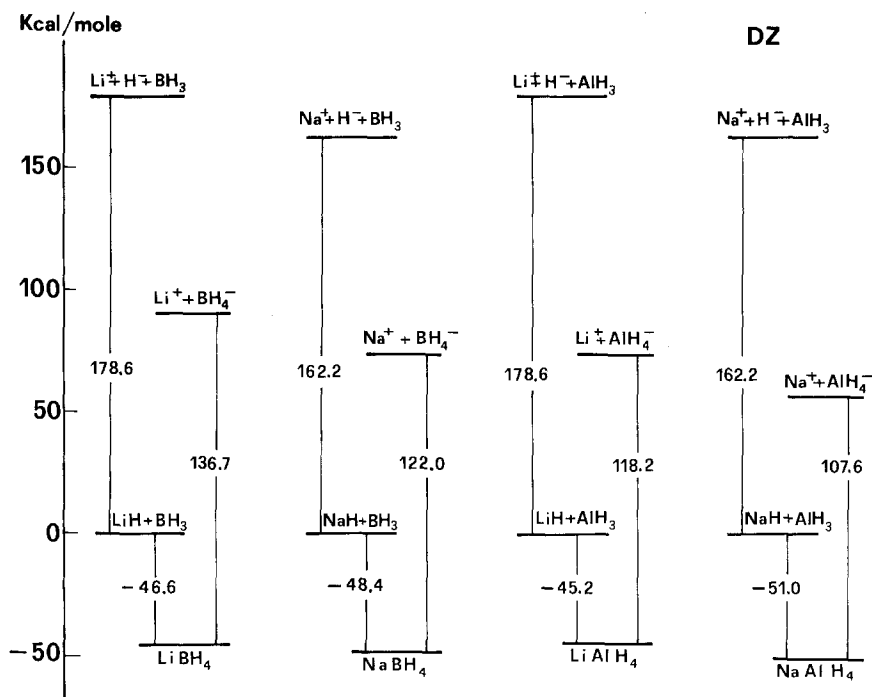


Fig. 7. Diagrams of the energies involved in the heterolytic dissociations of the Y—H bonds (DZ calculations)

The stabilization energy of the complex hydrides with respect to the separate partners YH and XH_3 is remarkably constant along the whole set (we note in passing that such a result heavily depends on the optimization of the YXH_4 geometries with the DZ basis) and the energies of the heterolytic cleavages, measured from the complex hydrides, indicate again that such processes, in gas phase conditions, are easier in the Al containing hydrides than in the B containing ones.

References

1. Eliel, E. L., Senda, Y.: *Tetrahedron* **26**, 2411 (1970)
2. Wigfield, D. C., Phelps, D. J.: *Can. J. Chem.* **50**, 388 (1972)
3. Brown, H. C., Ichikawa, K.: *J. Am. Chem. Soc.* **83**, 4372 (1961)
4. Ashby, E. C., Boone, J. R.: *J. Am. Chem. Soc.* **98**, 5524 (1976)
5. Wigfield, D. C., Gowland, F. W.: *Tetrahedron Letters* **38**, 3373 (1976)
6. Dill, J. D., Schleyer, P. v. R., Binkley, J. S., Pople, J. A.: *J. Am. Chem. Soc.* **99**, 6159 (1977)
7. Boldyrev, A. I., Charkin, D. P., Rambidi, N. G., Avdeev, V. I.: *Chem. Phys. Letters* **44**, 20 (1976)
8. Hehre, W. J., Lathan, W. A., Ditchfield, R., Newton, M. D., Pople, J. A.: *Gaussian 70*, Q.C.P.E., 236
9. Hehre, W. J., Stewart, R. F., Pople, J. A.: *J. Chem. Phys.* **51**, 2657 (1969)
10. Huzinaga, S., Arnau, C.: *J. Chem. Phys.* **52**, 2224 (1970)
11. Scrocco, E., Tomasi, J.: *Advan. Quantum Chem.* **11**, 115 (1978)

12. Bonaccorsi, R., Scrocco, E., Tomasi, J.: J. Am. Chem. Soc. **98**, 4049 (1976)
13. Morokuma, K.: J. Chem. Phys. **55**, 1236 (1971)
14. Kitaura, K., Morokuma, K.: Intern. J. Quantum Chem. **10**, 329 (1976)
15. Umeyama, H., Morokuma, K.: J. Am. Chem. Soc. **99**, 1316 (1977)
16. Kollman, P.: J. Am. Chem. Soc. **99**, 4875 (1977)
17. Perahia, D., Pullman, A., Pullman, B.: Theoret. Chim. Acta (Berl.) **43**, 207 (1976)
18. Scrocco, E., Silla, E., Tomasi, J.: Theoret. Chim. Acta (Berl.) **40**, 343 (1975)
19. Alagona, G., Scrocco, E., Silla, E., Tomasi, J.: Theoret. Chim. Acta (Berl.) **45**, 127 (1977)
20. Alagona, G., Scrocco, E., Tomasi, J.: Theoret. Chim. Acta (Berl.) **47**, 133 (1978)
21. Cade, P., Huo, W. J.: J. Chem. Phys. **47**, 649 (1967)
22. Clementi, E., Roetti, C.: At. Data Nucl. Data Tables **14**, 177 (1974)
23. Moore, C. E.: Atomic Energy Levels, Natl. Bur. Stds. Circ. 467 (U.S. GPO, Washington, D.C., 1949)

Received November 6, 1978/January 2, 1979